Int. J. Electrochem. Sci., 17 **(2022)** Article Number: 221232, doi: 10.20964/2022.12.34

International Journal of
ELECTROCHEMICAL
SCIENCE
www.electrochemsci.org

Molecularly imprinted electrochemical sensor based on g-C_3N_4 for determination of endosulfan insecticide in Agricultural Food

Chao Ma[1], *Duanpu Wu*[1], *Erjuan Xu*[1], *Ying Fan*[2,*]

[1] School of Chemical and Material Engineering, Guiyang University, Guiyang, 550005, China
[2] School of Horticulture, Shanxi Agricultural University, Taigu, 030800, China
[*]E-mail: yingfansxu@sina.com

Received: 12 September 2022 / *Accepted:* 21 October 2022 / *Published:* 30 November 2022

The goal of this research was to create an electrochemical sensor for endosulfan (EDS) insecticide and acaricide in agricultural food samples using a molecularly imprinted polymer (MIP) and a g-C_3N_4 nanostructure. For the synthesis of MIP/g-C_3N_4 nanocomposite on glassy carbon electrode (GCE), a direct decomposition method was used to synthesize g-C_3N_4, which was then used to modify the GCE surface, and MIP was prepared from 3-aminopropyl triethoxysilane, tetraethyl ortho-silicate, and EDS was used to modify the g-C_3N_4/GCE. According to structural analyses of modified electrodes, polymer nanoparticles with porous structures were dispersed on the sheet structure of g-C_3N_4, forming new rough nanocomposite after polymerization reactions. Electrochemical measurements using CV and DPV techniques revealed a highly sensitive and selective determination of EDS with a linear ranging from 0 to 96 μM and a limit of detection of 20 nM, indicating that MIP/g-C_3N_4/GCE as an EDS sensor performed similarly or even better than other reported EDS sensors in the literature. The capability of the MIP/g-C_3N_4/GCE for determining EDS in real samples prepared from celery samples was investigated, and analytical results showed that RSD values were less than 4.51% and recovery values were greater than 99.33%, indicating valid and accurate practical analyses in food in agricultural samples using the proposed EDS sensor.

Keywords: Electrochemical Sensor; Endosulfan; Molecularly Imprinted Polymer; g-C_3N_4; Nanocomposite; Agricultural food

1. INTRODUCTION

Endosulfan (EDS, $C_9H_6Cl_6O_3S$) is a compound composed of two stereoisomers, alpha-EDS and beta-EDS [1]. EDS is a hexachlorocyclopentadiene derivative that is chemically similar to aldrin, chlordane, and heptachlor [2, 3]. It is created by the Diels-Alder reaction of hexachlorocyclopentadiene with cis-butene-1,4-diol, followed by the reaction of the adduct with

thionyl chloride. EDS is commonly known by its trade name, Thiodan, and it is an organochlorine insecticide and acaricide that is widely used on coffee, tea, and cotton crops, among others [4, 5].

EDS can harm humans when inhaled and can be absorbed through the skin. High levels of EDS exposure can result in headaches, giddiness, blurred vision, nausea, vomiting, diarrhea, and muscle weakness [6]. Convulsions and coma may result from severe poisoning. According to reports, spraying EDS for crops has killed over 5000 people [7, 8]. It has also resulted in physical deformities among the locals. Because of its acute toxicity, bioaccumulation potential, and role as an endocrine disruptor, it has become a highly contentious agrichemical that is being phased out globally. Because of the risks to human health and the environment, it was banned by the Stockholm Convention in 2011 [9]. It's still in use in India, China, and a few other places [10, 11]. Victims of EDS poisoning are still born with deformities, mental or physical disorders, or other severe health complications, despite the pesticide being banned worldwide since 2011.

Pesticide residues left in the soil from previous applications pollute water bodies through runoff and leaching, eventually contaminating drinking water sources and contaminating agricultural food and wastewater. As a result, the development of an EDS sensor for determining RDS levels in food and agricultural wastewater samples is required, and several studies on spectrophotometry [12], gas chromatography–tandem mass spectrometry [13], enzyme immunoassay [14], high performance liquid chromatography [15], enzyme-linked immunosorbent assay [16], and electrochemical sensor [17-19] have been conducted. However, a variety of substances found in food and agricultural samples may act as potential interference compounds in the determination of EDS [20-22]. As a result, increasing sensor selectivity is an important factor in identifying and determining EDS levels in actual samples. Electrochemical sensors based on molecularly imprinted polymers (MIPs) are a growing class of synthetic materials that mimic molecular recognition by natural receptors [23, 24]. Non-covalent imprinting, which has no restrictions on the size, shape, or chemical character of the imprinted molecule, has the potential to produce tailor-made, highly selective artificial receptors with good mechanical, thermal, and chemical properties at a low cost [23, 25-27]. As a result, the goal of this research was to create an electrochemical sensor for EDS insecticide and acaricide in food samples using MIP and g-C_3N_4 nanostructures [28]. The novelty and advantage of the work is represented by the development of a new molecular imprinted polymer that could enhance the accessibility of the target species to the imprinted cavities and thus improve the selectivity of the MIPs as EDS sensors in a food sample.

2. MATERIALS AND METHODS

2.1. Synthesis of nanocomposite of MIP/g-C_3N_4 on GCE

First, a direct decomposition method was used for the synthesis of bulk g-C_3N_4 [29]. 1g of melamine (99%, Sigma-Aldrich) was put into a covered ceramic crucible and heated to 550 °C for 120 minutes with a heating rate of 5 °C/min under an atmospheric environment. After cooling, the synthesized g-C_3N_4 powder was milled and collected. Under condensation reaction of melamine, the discrete oligomers of melamine were converted to polymers and formed extended graphitic plane

networks which contained tri-s-triazine units building units connected with planar amino groups [30]. After that, 100 mg of bulk g-C_3N_4 was added to a mixture solution containing an equal volume ratio of H_2SO_4: HNO_3. The mixture was magnetically stirred for 8 hours. The suspension was then transferred to a Tefon-line autoclave and heated at 180 °C for 10 hours. The obtained powder was used for modification of the clean GCE surface. The 5 mL of 15µL g-C_3N_4 suspension was dropped on the GCE surface and the solution was evaporated under infrared lamp (Haining Sailing Electrical Appliance Co., Ltd., China). For fabrication of MIP/g-C_3N_4/GCE [31], the electrode was immersed in a mixture of 100 mM 3-aminopropyl triethoxysilane (≥98%, Sigma-Aldrich) as functional monomers and 50 mM tetraethyl ortho-silicate (98%, Sigma-Aldrich) as a cross linker in the presence of 25 mM EDS (Sigma-Aldrich) as template molecules. After 3 hours, the modified MIP/g-C_3N_4/GCE were dipped in ethanol (99%, Shandong Pulisi Chemical Co., Ltd., China) for 10 minutes to remove the EDS template. Then, the electrode was dried at room temperature. As a control, the NIP electrode was also prepared in the same procedure, but without adding the EDS template. Finally, the modified electrodes were stored in a refrigerator at 4 °C.

2.2. Characterizations

Structural and morphological analyses of synthesized samples were performed using Scanning electron microscopy (SEM; JEOL JSM-6390, Japan) and X-ray diffractometer (XRD; Bruker D8 Advanced difractometer, AXS, Karlsruhe, Germany). Cyclic voltammetry (CV) and differential pulse voltammetry (DPV) techniques were used for electrochemical analyses which were conducted on an electrochemistry workstation (CHI 660E, Chenhua Technology Co., Ltd., Shanghai, China) which contained a 3-electrodes cell, with a platinum plate electrode as a counter-electrode, an Ag/AgCl as reference electrode and modified or unmodified GCE as working electrode. The electrochemical analyses were carried out in 0.1 M Britton–Robinson buffer (BRB, Sigma-Aldrich) solution with pH 4.0. The pH of solutions was adjusted by the addition of 0.1 M HCl (37%, Merck Millipore, Germany) and 0.1 M NaOH (≥97.0%, Sigma-Aldrich).

2.3. Actual sample preparation

To investigate the capability of the EDS sensor in actual samples, celery samples were prepared as follows: celery samples were obtained from a local market and washed. A juicer was used to crush the samples. The obtained juice was filtered and centrifuged at 1000 rpm for 10 minutes to separate the liquid phase from the solid phase. The supernatant produced was used to prepare the real sample. The 0.001 mg/mL EDS (2.45 µM) was obtained by adding 0.2 mg of EDS solution to 100.0 mL of the resultant supernatant and 100.0 mL of 0.1 M RBR solution. For 10 minutes, the mixture was stirred in an ultrasonic bath. The standard method was also used to analyze the actual sample.

3. RESULTS AND DISCUSSION

3.1. Structural analyses of modified electrodes

Figure 1 exhibits the SEM micrographs of g-C_3N_4/GCE, MIP/g-C_3N_4/GCE and NIP/g-C_3N_4/GCE. As seen from the SEM micrograph of g-C_3N_4/GCE in Figure 1a, there is a sheet structure with a thin thickness which could provide a large surface area. The SEM micrographs for MIP/g-C_3N_4/GCE and NIP/g-C_3N_4/GCE (Figures 1b and 1c) show that after polymerization reactions, polymer nanoparticles can be evenly dispersed on the nanostructured surface of g-C3N4, forming new rough shapes of nanocomposite. The polymer layer in the MIP modified electrode has a porous structure due to the formation of cavities after the template is removed from the polymer layer. The structure of the NIP modified electrode is smooth. These porous MIP/g-C_3N_4/GCE structures are important for selective recognition of EDS molecules and indicate that the molecular imprinting surface was successfully prepared during polymerization reactions [32-34].

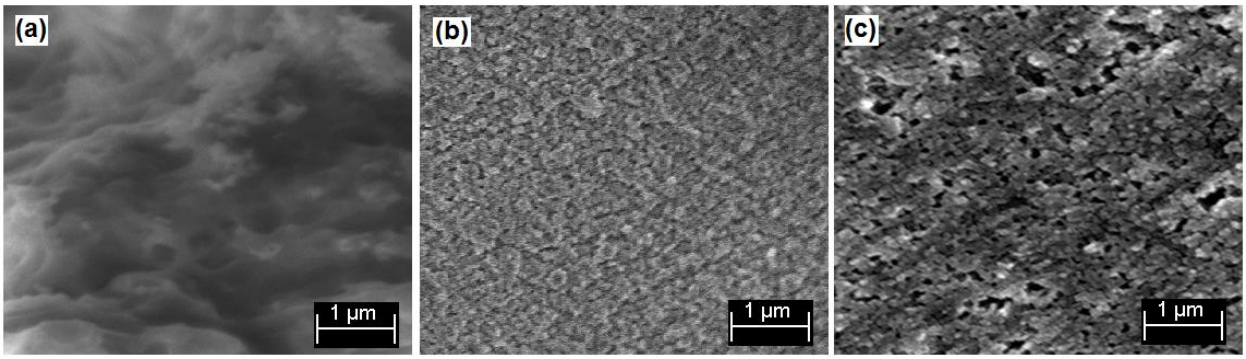

Figure 1. SEM micrographs of modified electrodes (a) g-C_3N_4/GCE, (b) MIP/g-C_3N_4/GCE and (c) NIP/g-C_3N_4/GCE.

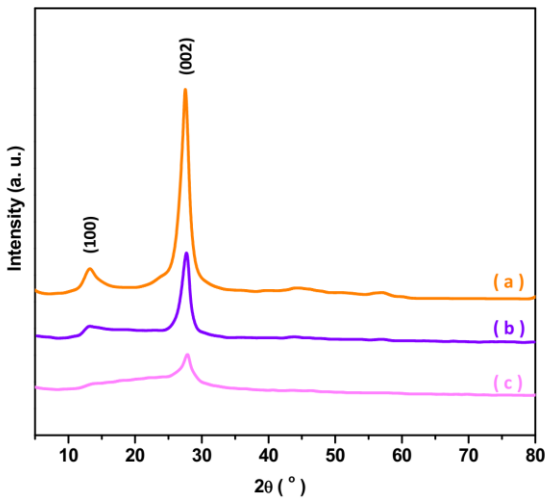

Figure 2. XRD of powders of (a) g-C_3N_4, (b) MIP/g-C_3N_4 and (c) NIP/g-C_3N_4.

Figure 2 depicts the XRD of powders of g-C_3N_4, MIP/g-C_3N_4 and NIP/g-C_3N_4. As seen from the XRD pattern of g-C_3N_4, there are two characteristic diffraction peaks at 2θ = 13.24° assigned to (100) Bragg reflection plane corresponding to the lattice planes parallel to the *c*-axis, and a diffraction peak is at 2θ = 27.38° which indexed to (002) plane of the interplanar stacking peak of the aromatic system of g-C_3N_4 [35-37]. According to the XRD patterns of MIP/g-C_3N_4 and NIP/g-C_3N_4, there is the same diffraction peak of the g-C_3N_4 inter-layer structure but with a lower intensity, and the peak at 2θ = 13.24° has disappeared in the MIP sample, which could be related to the formation of the porous structure in MIP/g-C3N4, which is consistent with the SEM results [38, 39].

3.2. Electrochemical measurements

Figure 3 displays the CV curves of MIP/g-C_3N_4/GCE, NIP/g-C_3N_4/GCE, g-C_3N_4/GCE and GCE in the potential range between -1.25 to 0.00 V at scan rate of 25 mV/s in 0.1 M BRB pH 4 containing 40 µM EDS. As seen, GCE does not show any redox peak, and there are the anodic peaks at -0.90 V, -0.93 V and -0.94 V at the CV curves of MIP/g-C_3N_4/GCE, NIP/g-C_3N_4/GCE and g-C_3N_4/GCE, respectively, that can be attributed to reducton EDS thruoght the formation of radical as a result of the reduction of the chlorine atom connected to the carbon in EDS that involves only one electron, and the second step involving one more proton and electron as shown in Figure 4 [18].

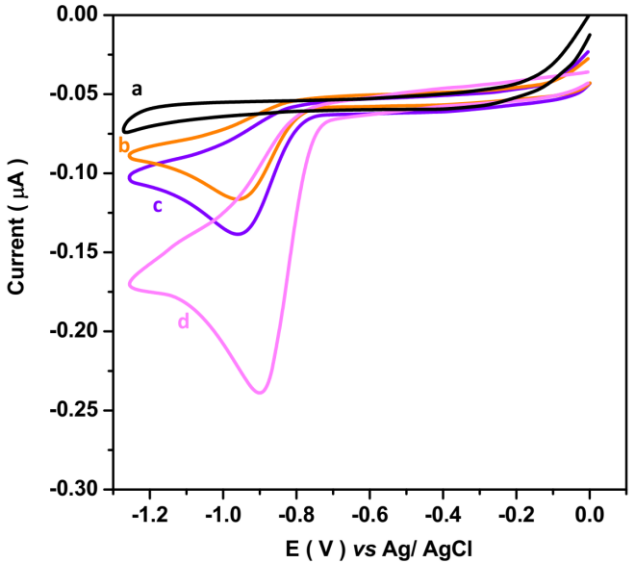

Figure 3. The CV curves of (a) GCE, (b) g-C_3N_4/GCE, (c) NIP/g-C_3N_4/GCE and (d) MIP/g-C_3N_4/GCE in potential range between −1.25 to 0.00 V at scan rate of 25 mV/s in 0.1 M BRB pH 4 containing 40 µM EDS.

As depicted, the CV curve of MIP/g-C_3N_4/GCE in Figure 3 shows the highest peak current of the all electrodes, and the cathodic peak is observed at an appreciably lower potential. It indicates to remarkably enhanced MIP/g-C_3N_4/GCE electrocatalytic performance because of the porous structure and large specific surface area of g-C_3N_4 which provide fast charge transfer and rich active sites [40-

42]. Furthermore, it can be related to MIP which is based on the measurement of the redox currents of template molecules that rebind with the cavities directly [43-45]. MIP is obtained by polymerizing EDS as template molecules with functional monomers through non-covalent or covalent bonds and eluting the template molecules which provide high selectivity for the empty cavities in the polymer structures and these cavities are complementary to the template molecule in size, shape, and functionality [46-48].

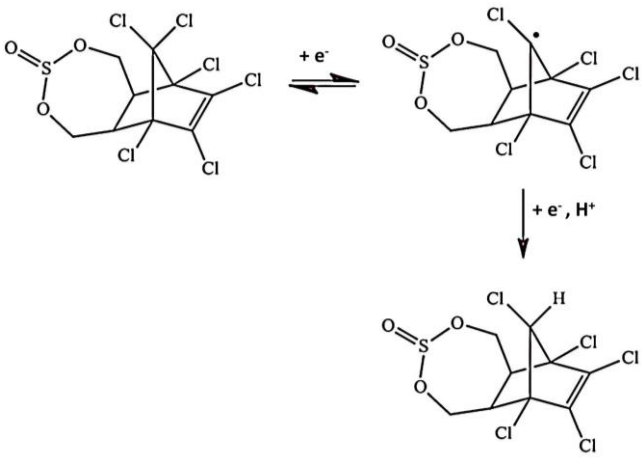

Figure 4. The suggested electrochemical reductoion mechanism of EDS [18].

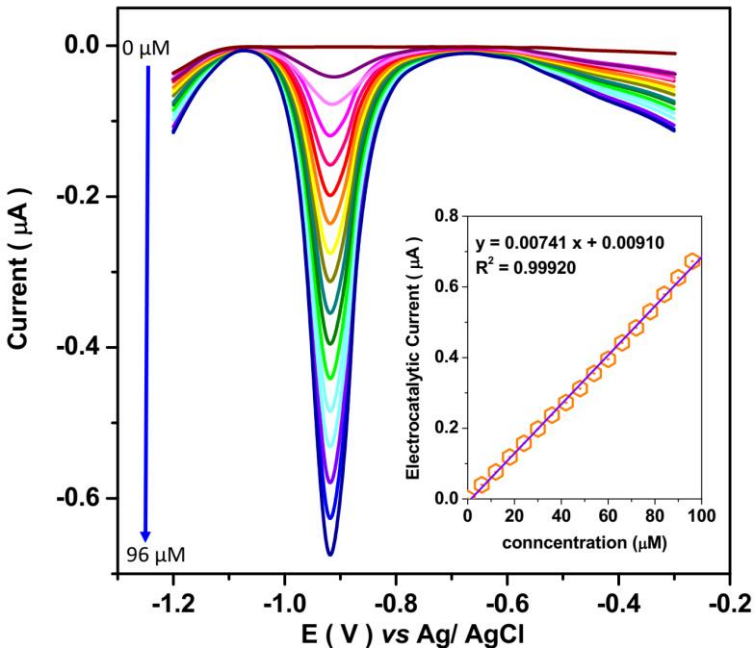

Figure 5. The DPV curves and related calibration plot of MIP/g-C_3N_4/GCE through consecutive addition of a solution containing 6 µM EDS in electrolyte of electrochemical cell (0.1 M BRB pH 4) under applied in potential between −1.2 to −0.3 V at scan rate of 25 mV/s.

Furthermore, MIPs have a higher connection capacity than NIPs because the resulting patterns of template molecules are not used in the NIP formation process [5, 49]. The basic interplay involved in the retention is ionic interaction, hydrogen bonds, and hydrophobic patches in addition to the shape formations in cavities. Thus, these interactions can further absorb template molecules on the MIP and it is more selective and has more capacity than NIP [50, 51]. As a result, the MIP-based sensor can improve template molecue sensitivity, selectivity, and adsorption efficiency [52, 53]. Therefore, the further electrochemical studies for the determination of EDS were performed using MIP/g-C_3N_4/GCE.

Table 1. Comparision between the MIP/g-C_3N_4/GCE sensing performance and the recent reported EDS sensors in literetures.

Electrode	Technique	LOD (nM)	Linear range (µM)	Ref.
MIP/g-C_3N_4/GCE	DPV	20	0 to 96	Current study
CuO microspheres	DPV	8.30	0.004 to 0.020	[17]
Fe_3O_4/f-MWCNT/ GCE	DPV	3300	0.1 to 20	[19]
MWCNT/antimony oxide/polyaniline/GCE	DPV	6800	32.3 to 77.6	[18]
NiO/GCE	DPV	0.17	0.05 to 25	[54]
C18/carbon paste electrode	DPV	0.098	---	[55]
Mercury film/GCE	SWV	59	0.05 to 10	[56]
Hanging mercury drop electrode	SWV	297	0.154 to 15.7	[57]
Antibody/Ferrocenedimethylamine /SWNTs	SWV	0.02	2×10^{-5} to 0.0491	[58]

SWV: square wave voltammetry

Figure 5a indicates the DPV curves and related calibration plot of MIP/g-C_3N_4/GCE through consecutive addition of a solution containing 6 µM EDS in the electrolyte of the electrochemical cell (0.1 M BRB pH 4) at an applied potential between -1.2 to -0.3 V at a scan rate of 25 mV/s. As seen, there is an increase in DPV peak current after each addition of an EDS solution. The DPV peak current is linearly increased by increasing the EDS concentration in the electrochemical cell from 0 to 96 µM. The sensitivity of MIP/g-C_3N_4/GCE can be determined to be 0.00741 µA/µM, and limit of detection is obtained to be 20 nM. Table 1 compares the MIP/g-C_3N_4/GCE sensing performance to that of recently reported EDS sensors in the literature. As found, the proposed EDS sensor in the current study reveals the wide linear range and appropriate limit of detection value toward the other reported EDS sensors which are related to the formation of 3D complementary cavities within the MIP on high porous surface of g-C_3N_4 nanostructure with the high electrocatalytic activity and the great specific surface area that it can act as an appropriate platform for immobilizaton of MIP cavities in sensor design [59-61].

The selectivity of the MIP/g-C_3N_4/GCE as an EDS sensor was studied in the presence of some chemicals and electroactive organic compounds as interference species in food samples and pesticides in agricultural samples. The results of DPV measurements using MIP/g-C_3N_4/GCE upon consecutive

additions of a solution containing 100 μM EDS and 500 μM interference substances solutions in 0.1 M BRB (pH 4.0) under applied potential between −1.2 to −0.3 V at scan rate of 25 mV/s are tabulated in Table 2. Results reveals that there is significant electrocatalytic current after addition of EDS solution in electrochemical cells, and addition of interference substances in electrolyte solution cannot remarkably change the electrocatalytic current, implying great selectivity of the MIP/g-C_3N_4/GCE in the determination of EDS in food and agricultural samples. This specificity can be attributed to the recognition mechanism of MIPs that it is mainly related to binding sites between template and monomer and the shape and rigidity of the template [62, 63].

Table 2. The results of DPV measurements using MIP/g-C_3N_4/GCE upon consecutive additions of a solution containing 100 μM EDS and 500 nμM interference substances solutions in 0.1 M BRB (pH 4.0) under applied in potential between −1.2 to −0.3 V at scan rate of 25 mV/s.

Substance	**Added (μM)**	**Amperometric signal (μA) at -0.90 V**	**RSD**
EDS	100	0.7412	±0.0085
Lindane	500	0.0338	±0.0011
Glucose	500	0.0416	±0.0017
Propazine	500	0.0109	±0.0011
Cyclohexane	500	0.0661	±0.0021
Trichlorfon	500	0.0636	±0.0019
Chlorpyrifos	500	0.0893	±0.0021
Triazophos	500	0.0494	±0.0018
Aminocarb	500	0.0570	±0.0019
Warfarin	500	0.0761	±0.0011
Fenitrothion	500	0.0674	±0.0010
Phenol	500	0.0490	±0.0019
Carbofuran	500	0.0376	±0.0017
Benzene	500	0.0575	±0.0015
SO_4^{2-}	500	0.0451	±0.0011
CO_3^{2-}	500	0.0722	±0.0013
HCO_3^-	500	0.0374	±0.0011
Mg^{2+}	500	0.0281	±0.0012
Fe^{2+}	500	0.0384	±0.0016
Pb^{2+}	500	0.0464	±0.0010
Cd^{2+}	500	0.0364	±0.0014

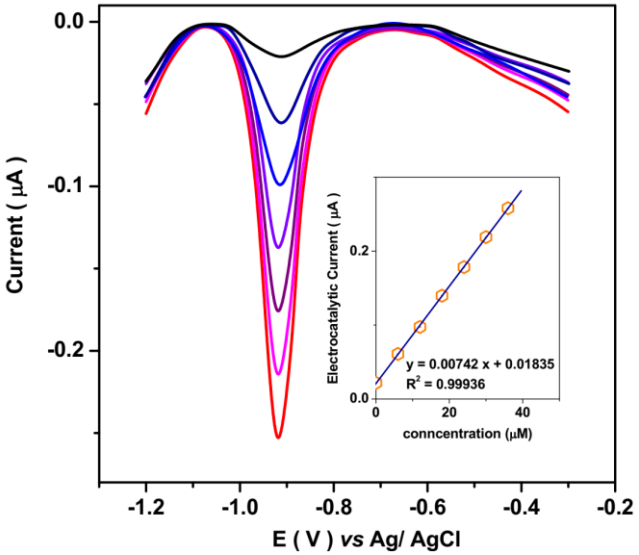

Figure 6. The DPV curves and related calibration plot of MIP/g-C_3N_4/GCE through consecutive addition of a solution containing 6 μM EDS in 0.1 M BRB pH 4 solution prepared from celery sample.

The MIP/g-C_3N_4/GCE capability for determination of EDS in real samples prepared from celery samples was examined. Figure 6 shows the DPV curves and related calibration plot of MIP/g-C_3N_4/GCE through consecutive addition of a solution containing 6 μM EDS in a 0.1 M BRB pH 4 solution prepared from a celery sample. The calibration graph demonstrates that the EDS level in the processed sample is 2.47 μM that it is very close to the EDS concentration in the preparation of real sample prosess (2.45 μM). Table 3 shows the analytical results which illustrates that the values of RSD are less than 4.51% and recovery values are more than 99.33%, indicating the validity and accuracy of practical analyses in food in agricultural samples using the proposed EDS sensor.

Table 3. Analytical applicability of MIP/g-C_3N_4/GCE to determine EDS in real samples.

Adding(μM)	Found(μM)	Recovery (%)	RSD (%)
6.00	5.96	99.33	3.32
12.00	11.93	99.41	3.76
18.00	17.93	99.61	4.51
24.00	23.92	99.66	4.24

4. CONCLUSION

The current study was carried out to design an electrochemical sensor for EDS in food samples using a MIP/g-C_3N_4 nanocomposite. For the synthesis of MIP/g-C_3N_4 nanocomposite on GCE, a direct decomposition method was used first, and then the MIP was prepared from 3-aminopropyl triethoxysilane, tetraethyl ortho-silicate, and EDS was modified to the g-C_3N_4/GCE. Structural

analyses of modified electrodes revealed that porous polymer nanoparticles were dispersed on the sheet structure of g-C_3N_4, forming new rough shapes in nanocomposite after polymerization reactions. Electrochemical studies demonstrated highly sensitive and selective EDS determination with a linear ranging from 0 to 96 μM and a detection limit of 20 nM. The capability of the MIP/g-C_3N_4/GCE for determining EDS in real samples prepared from celery samples was investigated, and analytical results indicated valid and accurate practical analyses in food in agricultural samples using the proposed EDS sensor.

ACKNOWLEDGEMENT
This work was sponsored in part by Guiyang science and technology plan project (Zhuke contract (2021) No. 43-17); Guiyang university teaching reform project (No. 2021244).

References

1. I. Mukherjee and M. Gopal, *Toxicological & Environmental Chemistry*, 46 (1994) 217.
2. N. Vivekanandhan and A. Duraisamy, *Universal Journal of Environmental Research & Technology*, 2 (2012) 369.
3. A.E. Anqi, C. Li, H.A. Dhahad, K. Sharma, E.-A. ATTIA, A. Abdelrahman, A.G. Mohammed, S. Alamri and A.A. Rajhi, *Journal of Energy Storage*, 52 (2022) 104906.
4. G. He, X. Liu and Z. Cui, *Global Food Security*, 29 (2021) 100536.
5. R. Kumar, N. Ranjan, V. Kumar, R. Kumar, J.S. Chohan, A. Yadav, S. Sharma, C. Prakash, S. Singh and C. Li, *Journal of Materials Engineering and Performance*, 31 (2022) 2391.
6. G.L. Tadesse and T. Kasa, *Advances in Life Science and Technology*, 55 (2017) 13.
7. B. Dinham and S. Malik, *International journal of occupational and environmental health*, 9 (2003) 40.
8. X. Li, X. Yue, Q. Huang and B. Zhang, *Carbohydrate Polymers*, 284 (2022) 119176.
9. A. Casanova, S. Cabrera, G. Díaz-Ruiz, S. Hernández, C. Wacher, M. Zubillaga and I. Ortíz, *Folia Microbiologica*, 66 (2021) 973.
10. Y. Yang, M. Yang, C. Li, R. Li, Z. Said, H.M. Ali and S. Sharma, *Frontiers of Mechanical Engineering*, (2022) 1.
11. C. Liu and J. Rouhi, *RSC Advances*, 11 (2021) 9933.
12. C. Pasha and B. Narayana, *Bulletin of environmental contamination and toxicology*, 80 (2008) 85.
13. J.M. Vidal, F. Arrebola, A. Fernández-Gutiérrez and M. Rams, *Journal of Chromatography B: Biomedical Sciences and Applications*, 719 (1998) 71.
14. R.M. Dreher and B. Podratzki, *Journal of agricultural and food chemistry*, 36 (1988) 1072.
15. M. Pirsaheb, N. Fattahi, F. Amirian and K. Sharafi, *Journal of Analytical Chemistry*, 74 (2019) 114.
16. N. Lee, J.H. Skerritt and D.P. McAdam, *Journal of Agricultural and Food Chemistry*, 43 (1995) 1730.
17. S.S. Rathnakumar, K. Noluthando, A.J. Kulandaiswamy, J.B.B. Rayappan, K. Kasinathan, J. Kennedy and M. Maaza, *Sensors and Actuators B: Chemical*, 293 (2019) 100.
18. K.K. Masibi, O.E. Fayemi, A.S. Adekunle, A.M. Al-Mohaimeed, A.M. Fahim, B.B. Mamba and E.E. Ebenso, *Materials*, 14 (2021) 723.
19. G. Uwaya, N.J. Gumede and K. Bisetty, *ACS Omega*, 6 (2021) 30515.
20. Y. Sun, J. Li, L. Zhu and L. Jiang, *Current Opinion in Food Science*, 44 (2022) 100813.

21. X. Wang, C. Li, Y. Zhang, H.M. Ali, S. Sharma, R. Li, M. Yang, Z. Said and X. Liu, *Tribology International*, 174 (2022) 107766.
22. L. Nan, C. Yalan, L. Jixiang, O. Dujuan, D. Wenhui, J. Rouhi and M. Mustapha, *RSC Advances*, 10 (2020) 27923.
23. M. Blanco-López, M. Lobo-Castañón, A. Miranda-Ordieres and P. Tunon-Blanco, *TrAC Trends in Analytical Chemistry*, 23 (2004) 36.
24. B. Liu, Y. Ma, F. Zhou, Q. Wang and G. Liu, *International Journal of Electrochemical Science*, 15 (2020) 9590.
25. A.A. Lahcen and A. Amine, *Electroanalysis*, 31 (2019) 188.
26. M. Pohanka, *International Journal of Electrochemical Science*, 12 (2017) 8082.
27. M. Wang, B. Gao, Y. Xing and X. Xiong, *International Journal of Electrochemical Science*, 15 (2020) 8437.
28. J. Rouhi, H.K. Malayeri, S. Kakooei, R. Karimzadeh, S. Alrokayan, H. Khan and M.R. Mahmood, *International Journal of Electrochemical Science*, 13 (2018) 9742.
29. J. Fu, B. Zhu, C. Jiang, B. Cheng, W. You and J. Yu, *Small*, 13 (2017) 1603938.
30. Z. Yang, X. Xu, X. Liang, C. Lei, Y. Cui, W. Wu, Y. Yang, Z. Zhang and Z. Lei, *Applied catalysis B: environmental*, 205 (2017) 42.
31. J. Hassanzadeh, B.R. Moghadam, A. Sobhani-Nasab, F. Ahmadi and M. Rahimi-Nasrabadi, *Spectrochimica Acta Part A: Molecular and Biomolecular Spectroscopy*, 214 (2019) 451.
32. W.J. Cheong, F. Ali, J.H. Choi, J.O. Lee and K.Y. Sung, *Talanta*, 106 (2013) 45.
33. Q. Xie, G. Liu, Y. Zhang, J. Yu, Y. Wang and X. Ma, *Critical Reviews in Food Science and Nutrition*, (2022) 1.
34. H. Karimi-Maleh, C. Karaman, O. Karaman, F. Karimi, Y. Vasseghian, L. Fu, M. Baghayeri, J. Rouhi, P. Senthil Kumar and P.-L. Show, *Journal of Nanostructure in Chemistry*, 12 (2022) 429.
35. T.H.T. Vinh, C.M. Thi and P. Van Viet, *Materials Letters*, 281 (2020) 128637.
36. A.M. Paul, A. Sajeev, R. Nivetha, K. Gothandapani, P. Bhardwaj, K. Govardhan, V. Raghavan, G. Jacob, R. Sellapan and S.K. Jeong, *Diamond and Related Materials*, 107 (2020) 107899.
37. X. Cui, C. Li, Y. Zhang, W. Ding, Q. An, B. Liu, H.N. Li, Z. Said, S. Sharma and R. Li, *Frontiers of Mechanical Engineering*, 18 (2023) 1.
38. C. Zhang, J. Liu, X. Huang, D. Chen and S. Xu, *ACS Omega*, 4 (2019) 17148.
39. D. Zhenjing, L. Changhe, Y. Zhang, D. Lan, B. Xiufang, Y. Min, J. Dongzhou, L. Runze, C. Huajun and X. Xuefeng, *Chinese Journal of Aeronautics*, 34 (2021) 33.
40. J. Yang, X. Zhang, C. Xie, J. Long, Y. Wang, L. Wei and X. Yang, *Journal of Electronic Materials*, 50 (2021) 1067.
41. H. Savaloni, E. Khani, R. Savari, F. Chahshouri and F. Placido, *Applied Physics A*, 127 (2021) 1.
42. R. Savari, J. Rouhi, O. Fakhar, S. Kakooei, D. Pourzadeh, O. Jahanbakhsh and S. Shojaei, *Ceramics International*, 47 (2021) 31927.
43. L. Zhang, J. Li and Y. Zeng, *Microchimica Acta*, 182 (2015) 249.
44. M. Liu, C. Li, C. Cao, L. Wang, X. Li, J. Che, H. Yang, X. Zhang, H. Zhao and G. He, *Food Engineering Reviews*, 13 (2021) 822.
45. Z. Duan, C. Li, Y. Zhang, M. Yang, T. Gao, X. Liu, R. Li, Z. Said, S. Debnath and S. Sharma, *Frontiers of Mechanical Engineering*, (2022) 1.
46. L. Zhang, G. Wang, C. Xiong, L. Zheng, J. He, Y. Ding, H. Lu, G. Zhang, K. Cho and L. Qiu, *Biosensors and Bioelectronics*, 105 (2018) 121.
47. Z. Said, S. Arora, S. Farooq, L.S. Sundar, C. Li and A. Allouhi, *Solar Energy Materials and Solar Cells*, 236 (2022) 111504.
48. H. Karimi-Maleh, R. Darabi, M. Shabani-Nooshabadi, M. Baghayeri, F. Karimi, J. Rouhi, M. Alizadeh, O. Karaman, Y. Vasseghian and C. Karaman, *Food and Chemical Toxicology*, 162 (2022) 112907.

49. Y. Zhang, D. Song, L.M. Lanni and K.D. Shimizu, *Macromolecules*, 43 (2010) 6284.
50. Z. Karimi Baker and S. Sardari, *Iranian Biomedical Journal* 25 (2021) 68.
51. X. Wang, C. Li, Y. Zhang, W. Ding, M. Yang, T. Gao, H. Cao, X. Xu, D. Wang and Z. Said, *Journal of Manufacturing Processes*, 59 (2020) 76.
52. L. Zhang, G. Wang, D. Wu, C. Xiong, L. Zheng, Y. Ding, H. Lu, G. Zhang and L. Qiu, *Biosensors and Bioelectronics*, 100 (2018) 235.
53. M. Yang, C. Li, Y. Zhang, Y. Wang, B. Li, D. Jia, Y. Hou and R. Li, *Applied Thermal Engineering*, 126 (2017) 525.
54. H. Bakhsh, J.A. Buledi, N.H. Khand, B. Junejo, A.R. Solangi, A. Mallah and S.T.H. Sherazi, *Journal of Food Measurement and Characterization*, 15 (2021) 2695.
55. H. El Bakouri, J.M. Palacios-Santander, L. Cubillana-Aguilera, A. Ouassini, I. Naranjo-Rodríguez and J.L.H.-H. de Cisneros, *Chemosphere*, 60 (2005) 1565.
56. M. Tefera, M. Tessema, S. Admassie and A. Guadie, *Sensing and Bio-Sensing Research*, 33 (2021) 100431.
57. F.W. Ribeiro, T.M. Oliveira, F.L. da Silva, G.L. Mendonca, P. Homem-de-Mello, H. Becker, P. de Lima-Neto, A.N. Correia and V.N. Freire, *Microchemical Journal*, 110 (2013) 40.
58. G. Liu, S. Wang, J. Liu and D. Song, *Analytical Chemistry*, 84 (2012) 3921.
59. Z. Savari, S. Soltanian, A. Noorbakhsh, A. Salimi, M. Najafi and P. Servati, *Sensors and Actuators B: Chemical*, 176 (2013) 335.
60. H. Savaloni, R. Savari and S. Abbasi, *Current Applied Physics*, 18 (2018) 869.
61. F. Chahshouri, H. Savaloni, E. Khani and R. Savari, *Journal of Micromechanics and Microengineering*, 30 (2020) 075001.
62. Y. Huang, J. Pan, Y. Liu, M. Wang, S. Deng and Z. Xia, *Analytical chemistry*, 91 (2019) 8436.
63. X. Cui, C. Li, Y. Zhang, Z. Said, S. Debnath, S. Sharma, H.M. Ali, M. Yang, T. Gao and R. Li, *Journal of Manufacturing Processes*, 80 (2022) 273.